Optimizing shared charging services at sustainable bus charging hubs: A queue theory integration approach

Renewable Energy 237 (2024) 121860

Contents lists available at ScienceDirect

Renewable Energy

journal homepage: www.elsevier.com/locate/renene

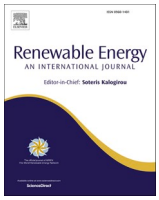

Optimizing shared charging services at sustainable bus charging hubs: A queue theory integration approach

Zhengke Liu [a], Xiaolei Ma [a,b], Siyu Zhuo [c,d], Xiaohan Liu [e,*]

[a] School of Transportation Science and Engineering, Beihang University, Beijing, 100191, China
[b] Key Laboratory of Intelligent Transportation Technology and System, Ministry of Education, Beijing, 100191, China
[c] School of Traffic and Transportation, Beijing Jiaotong University, Beijing, 100044, China
[d] Key Laboratory of Transport Industry of Comprehensive Transportation Theory (Beijing Jiaotong University), Ministry of Transport, Beijing, 100044, China
[e] Department of Architecture and Civil Engineering, Chalmers University of Technology, 41296, Göteborg, Sweden

ARTICLE INFO

Keywords:
Electric bus charging scheduling
Solar photovoltaic energy
Renewable energy on-site consumption
Shared charging mode
Optimization-based model
Queue theory

ABSTRACT

Integrating solar photovoltaic (PV) systems into bus charging infrastructure offers a promising solution to mitigate carbon emissions and reduce grid loads. However, a mismatch between the output of solar PV energy and the electric bus (EB) charging demand can arise due to the instability and intermittency of solar PV energy. To address this issue, this study introduces a novel shared charging business mode that allocates charging facilities to private electric vehicles (PEVs), leveraging idle infrastructure to maximize solar PV utilization. We develop an optimization framework to jointly determine the EB charging schedules and the allocation of charging facilities between EBs and PEVs within an EB network integrated with solar PV systems. Additionally, a loss queue model with time-dependent arrival rates is proposed to model the stochastic nature of PEV charging demand. A case study is conducted on a bus network in Beijing to validate our proposed operational strategy. The findings demonstrate that integrating shared charging in bus depots equipped with solar PV systems improves solar PV utilization from 79.30 % to 92.91 %. This integration reduces CO_2 emissions and overall daily system costs by 7.93 % and 14.82 %, respectively, without negatively impacting the grid load during peak periods.

1. Introduction

1.1. Motivation

The transportation industry, responsible for 26 % of global energy use, plays a critical role in climate change due to its substantial carbon emissions [1]. It is widely recognized that this sector urgently needs to reduce carbon emissions from internal combustion engine vehicles. Recently, the advancement of electric vehicles has emerged as a viable solution to mitigate energy pressures and meet dual carbon objectives, such as reaching peak carbon emissions by 2030 and achieving carbon neutrality by 2060 in China [2,3]. Consequently, governments worldwide are formulating policies to foster transportation electrification, including measures to substitute internal combustion engine vehicles with electric vehicles [4,5]. For instance, the Netherlands has decreed that all new passenger cars must be zero-emissions by 2030 [6]. Along this line, the electric bus (EB) stands out as a promising solution to curb carbon emissions and street-level air pollution associated with transportation in densely populated urban areas [7,8]. For example, by 2024, Beijing aims to have electric and clean energy buses that make up 94 % of its citywide fleet [9]. Similarly, the Land Transport Authority of Singapore has committed to achieving a fully electrified bus fleet by 2040 [10]. However, the widespread adoption of electric transportation could potentially result in increased overall carbon emissions if the electricity used is predominantly sourced from carbon-intensive methods [11].

Fortunately, the EB systems integrated with renewable energy have the potential to significantly reduce overall carbon emissions, particularly when the share of renewable energy in electricity generation exceeds a certain threshold level [11–14]. Rooftop photovoltaic (PV), which is one of the most significant renewable energy sources in urban areas, can be seamlessly integrated with charging facilities in bus depots [15]. Recent studies have explored integrating solar energy into urban EB/EV operations [16,17], highlighting that using rooftop PV for EB charging can effectively tackle air pollution and carbon emissions. However, the intermittent nature of solar energy can create mismatches

* Corresponding author.
E-mail address: xiaohanl@chalmers.se (X. Liu).

https://doi.org/10.1016/j.renene.2024.121860
Received 28 June 2024; Received in revised form 4 October 2024; Accepted 9 November 2024
Available online 12 November 2024

between solar PV output and EB charging demands [18,19], necessitating increased energy storage and impacting local grids [20]. Introducing energy storage systems is a straightforward solution to this challenge. There is growing interest in integrating photovoltaic and energy storage systems (PESS) into daily EB operations to optimize PV utilization [17,21,22]. However, it should be noted that incorporating energy storage batteries involves additional investments. This raises a critical challenge: How can transit agencies synchronize EB charging schedules to maximize solar PV energy on-site consumption without energy storage batteries?

EBs should shift their charging demand from nighttime to daytime hours to optimize the on-site consumption of solar PV energy. However, most EBs have busy daytime schedules with limited charging opportunities, resulting in underutilized charging facilities and wasted solar PV energy in bus depots. Therefore, the current operational strategy for EB systems does not effectively harness solar PV energy. Recently, a promising operational strategy for bus depots known as the shared charging mode has garnered scholarly attention. This mode allows private electric vehicles (PEVs) to use bus depot charging facilities for a fee during specified periods. Studies by Ye, Yu, Wei and Liu [23] and Ji, Bie and Wang [24] have addressed the deployment and scheduling problems of bus depots employing shared charging modes. Their findings illustrate that this mode can alleviate peak electricity demand, facilitate PEV charging without disrupting EB schedules, and generate additional revenue for public transport (PT) companies. Clearly, this shared strategy has the potential to improve solar PV energy on-site consumption by allocating charging facilities to PEVs, transforming their charging demand into additional consumption of solar PV output during the daytime, thereby compensating for the limited consumption capacity of EBs. From the perspective of PEV owners, the uneven distribution of public charging infrastructure presents a significant challenge in meeting their charging needs. On one hand, sharing idle charging piles with PEV owners can alleviate “charging anxiety” by increasing the availability of charging points. On the other hand, the charging facilities in EB depots are typically well-maintained and offer higher-quality charging services compared to many public charging stations. This can result in faster and more reliable charging for PEV owners, enhancing their overall user experience. Therefore, the shared charging mode has the potential to create a win-win situation: public transport operators benefit from improved utilization of their infrastructure and increased revenue, while PEV owners gain access to more dependable and widely available charging services.

However, no studies have explored the impact of shared charging modes on economic and environmental benefits or grid loads of bus depots equipped with solar PV systems within a bus network. To address this gap, this study proposed an optimization framework to jointly optimize EB charging schedules and the allocation of charging facilities between EBs and PEVs throughout the day, aiming to improve network-level on-site consumption of solar PV energy and reduce overall daily system costs.

1.2. Contributions

Based on the identified challenges and gaps in the literature, this study aims to provide a comprehensive solution. The key contributions are as follows:

- Developing a novel mathematical model that efficiently simulates the operations of a bus network integrating solar PV systems and a shared charging mode, while satisfying the constraints of dynamic battery state of charge (SoC) of EBs and the capacity of charging piles in bus depots. This model facilitates the decision-making process for EB charging schedules and the allocation of charging facilities between EBs and PEVs throughout the day.
- Formulating a loss queue model with time-dependent arrival rates to account for the stochastic nature of PEV charging demand. A numerical solution method is designed to efficiently solve the queue model and evaluate the performance of PEV charging states.
- Conducting a real-world case study of a bus network in Beijing integrating multi-source data such as operational data of EBs, charging demand data of PEVs, and temperature and irradiance data. Validating the effectiveness of sharing charging mode through a comparison analysis with two operational strategies without shared charging.

2. Literature review

2.1. EB charging scheduling with solar PV integration

There are several charging technologies for EBs, such as plug-in charging, inductive (wireless) charging, and battery swapping. At present, the most prevalent technology is plug-in charging, involving the connection of a cable to a charging pile. Given that this study utilizes plug-in charging technology for EBs, the literature review will concentrate on existing research on plug-in charging scheduling. Readers interested in other charging technologies can refer to Perumal, Lusby and Larsen [25], Manzolli, Trovão and Antunes [26], and Zhou, Wang, Wang, Yu and Tang [27]. During daily operations, a predetermined charging schedule is allocated to EBs for each trip. EBs can charge during intervals such as trip breaks or overnight periods. Recently, a substantial body of literature has employed optimization methods to address the scheduling of EB charging [8,28,29]. Nevertheless, integrating solar PV systems into the EB scheduling problem requires careful extension of the existing mathematical models to facilitate solutions. Zaneti, Arias, de Almeida and Rider [22] developed an optimization-based approach for managing EB charging schedules for a bus depot equipped with PESS on a university campus. A mixed-integer linear programming (MILP) model was formulated to improve the charging type as well as the charging time. Real-world case studies demonstrated a substantial decrease in operating costs, further enhanced by incorporating PESS. To address the issues of solar PV output uncertainty, Liu, Liu, Zhang, Zhou, Chen and Ma [21] proposed a two-stage stochastic programming to jointly optimize the location problem of bus depots equipped with PESS and the charging scheduling problem of EBs. The results demonstrated that the introduction of PESS can significantly reduce both the annual charging cost and carbon emissions. Ren, Ma, Fai Norman Tse, and Sun [30] proposed a MILP model to optimize the charging control of EBs at solar-powered bus depots without energy storage batteries, aimed at improving solar PV energy on-site consumption and minimizing reliance on the grid. Results indicated that optimal EB charging scheduling could considerably improve the on-site consumption ratio of solar PV energy and realize the similar performance of installing energy storage systems. Liu, Cathy Liu, Liu, Shi and Ma [31] formulated a two-stage robust optimization model to address disruptions in PESS and provide resilient EB charging scheduling. The results indicated that PESS can reduce daily bus charging costs and enhance the reliability of transportation services for passengers when interruptions occur in EB systems.

2.2. Shared charging strategy

The rising adoption of PEVs in urban regions, coupled with limited public charging facilities, results in a considerable discrepancy between charging demand and supply. Leveraging idle private charging infrastructure for PEVs presents a viable solution to mitigate the stress on public charging stations. The academic discussion on shared charging frameworks can be broadly divided into two categories: one involving the use of private home charging piles for PEVs and the other concerning the sharing of charging piles in bus depots with PEVs. In the shared charging scenario based on private home charging piles, the primary challenge lies in modeling the behavior of both private charging pile owners and PEV drivers due to the random nature of charging schedules. Plenter, Chasin, von Hoffen, Betzing, Matzner and Becker [32]

introduced a technology-enabled peer-to-peer sharing and collaborative consumption model for sharing non-public charging piles of private individuals and small enterprises with other PEV owners. Findings reveal that 36 % of German respondents indicated their willingness to offer charging services within such a theoretical marketplace. Chen, Huang, Cao, Li, Yan, Wu and Liang [33] transformed the shared charging facility allocation problem into a generalized Nash game. They proposed a hierarchical scheduling model for PEVs, which coordinates public charging stations and shared residential charging piles for PEV charging. Yang, Liu, Zhuge, Wong and Wang [34] examined the potential of sharing home charging piles in Beijing using a data-driven micro-simulation approach. The results suggest that this strategy could provide additional charging opportunities for PEV owners and lessen their dependence on public charging stations. Unlike the shared mode based on home charging piles, shared charging piles in bus depots should consider the scheduling of EBs, which presents a network-level analysis challenge. Ye, Yu, Wei and Liu [23] introduced a shared charging hub capable of providing charging services for both EBs and PEVs, using a spatio-temporal optimization model to optimize the deployment and operation of shared charging hubs with the aim of minimizing greenhouse gas emissions within financial constraints, while preventing significant spikes in peak power demand. Findings show that the shared charging hubs can lead to substantial reductions in greenhouse gas emissions while mitigating peak electricity demand. Ji, Bie and Wang [24] proposed a sharing strategy allowing EBs' charging piles to be used by PEVs and jointly optimized EB scheduling and charging infrastructure sharing. The model's optimization variables include the allocation of charging piles for EBs and PEVs within each time frame, as well as the daily assignment of specific trips and charging schedules for each EB. A real-world bus route is employed to validate the proposed optimization technique. Findings demonstrate that this charging infrastructure sharing strategy can facilitate PEV charging without disrupting EB schedules, thereby increasing revenue for public transportation firms. Jia, An and Ma [35] proposed a two-stage stochastic model to optimize the number of chargers and the distribution of charging power for PEVs, considering the uncertainty in EB and PEV charging demands and arrival times. A real-world case study of a bus depot in Shanghai is illustrated with 127 EBs and 376 PEVs. The results suggest that allocating half of the charging piles can satisfy nearly all PEV charging demands, thus generating a profit rather than a cost.

2.3. Summary and research gaps

In summary, previous studies on EB charging scheduling integrated with solar PV systems have primarily focused on mitigating the mismatch between EB charging demand and solar PV output through the implementation of energy storage systems, aimed at reducing the expense of solar abandonment. However, limited research has been conducted on optimizing EB charging schedules specifically to improve on-site consumption of solar PV energy. Regarding the shared charging facilities, current research has extensively analyzed the economic viability of shared facilities for PEVs. However, considering the limited consumption capacity of EBs to utilize solar PV energy during the daytime, the PEV charging demand presents an opportunity to balance the mismatch between EB charging demand and solar PV output. Thus, investigating the potential impact of the shared charging mode on the economic and environmental benefits of bus depots equipped with solar PV systems is crucial for PT operators. To the best of our knowledge, this issue remains unexplored in current literature.

The remainder of this paper is organized as follows: Section 3 presents the problem description and model formulation. Section 4 presents a real-world case study and analyzes the model results. Section 5 discusses the main findings and potential research directions.

3. Model formulation

3.1. Problem description

We consider a bus network including $|J|$ bus depots operated by a PT operator, which provides parking and charging services for a certain number of bus routes and EBs in a regional area. Unlike conventional bus depots, the depots in our studied network have fully installed solar PV systems to reduce lifetime carbon emissions (i.e., from plants to vehicles). To improve the network-level on-site consumption of solar energy and reduce the overall daily system cost, the PT operator decides to share charging piles with PEVs, leveraging idle charging piles to maximize solar PV utilization during the daytime. As illustrated in Fig. 1, each trip in the pre-designed EB schedule is assigned to an EB in advance. EBs can choose to charge during breaks between successive trips or overnight. The time-dependent solar PV output and PEV charging demand require the PT operator to develop operational schedules for EBs and allocation plans for charging facilities on a day-by-day basis. To mitigate the potential disruption caused by the occupation of charging piles by PEVs on EB operations, the specific number of charging piles available for PEVs should be limited [36]. The PT operator aims to jointly optimize EB charging scheduling and the allocation of charging facilities between EBs and PEVs over a day. It should be noted that we assume the PT operator adopts a smart charging system that allows centralized control over the allocated power for each charging pile, thereby controlling the charging start time and duration for each vehicle plugged in.

3.2. Mathematical model

3.2.1. Notation

Table 1 provides a comprehensive overview of the sets, indices, parameters, and variables utilized in the mathematical model, serving as a useful reference for readers.

3.2.2. Objective function

The objective is to minimize the total cost, which includes charging costs, carbon emission costs, and the revenues from solar PV systems and charging services provided to PEV owners, both of which are negative. Notably, the carbon emission costs from charging PEVs are borne by PEV owners themselves, regardless of the energy source.

$$min\ Z = \sum_{j\in J}\sum_{t\in T}\left[(c_t + c_{emis})Q_{j,t}\right] - \sum_{j\in J}\sum_{t\in T}\left[(c_t + c_{emis})u_{j,t} + (c_t + c_{emis})Q_{j,t}^{PEV}\right] \tag{1}$$

where, c_t and c_{emis} indicate the electricity price at time interval t and the cost of carbon emissions, respectively. $Q_{j,t}$ and $Q_{j,t}^{PEV}$ represent the total electricity consumption and the total electricity consumption of PEVs in bus depot j at time interval t, respectively. $u_{j,t}$ indicates the energy consumption of solar PV systems in bus depot j at time interval t.

The investment cost of solar PV systems is excluded from the objective function, as the PV panels are already fully installed on the available rooftop areas of bus depots. This setup provides an optimal infrastructure planning solution for PT operators, as daytime electricity prices consistently surpass the equivalent daily costs of installing and operating solar PV systems. Therefore, whether PT operators use PV power to charge EBs or sell electricity to PEV drivers, both options offer economic benefits. However, when calculating the overall daily system costs, it remains crucial to account for the investment and operational costs associated with solar PV systems to ensure a fair comparison of different operational strategies.

3.2.3. Constraints

(1) EB sector

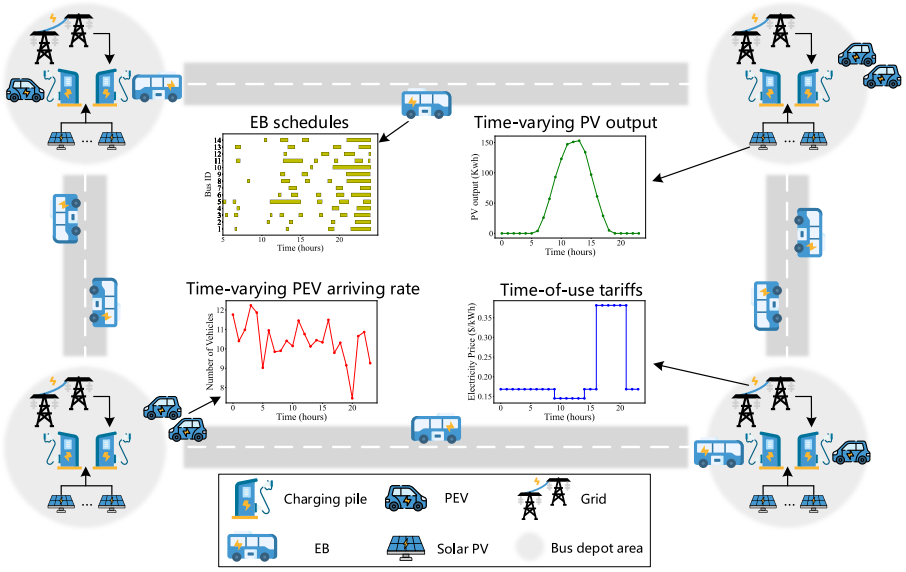

Fig. 1. Depiction of the investigated problem.

Let the continuous variables $E_{v,l}$ and $E'_{v,l}$ represent the remaining electricity in the battery of EB v before and after its l^{th} break, respectively. Constraints (2) and (3) regulate the monitoring of the remaining electricity in the battery of EB v throughout all its scheduled trips.

$$E_{v,l} = E'_{v,l-1} - e_{v,l}, \forall v \in V, \forall l \in L_v \tag{2}$$

Here, $e_{v,l}$ represents the accumulated electricity consumed by EB v in the trip before its l^{th} break.

$$E'_{v,l} = E_{v,l} + q_{v,l}, \forall v \in V, \forall l \in L_v \tag{3}$$

where, $q_{v,l}$ denotes the electricity charged for the EB v during its l^{th} break. It can be calculated by Equation (5).

We define the binary variable $x_{v,l,d(l),t}$ as follows. This variable indicates whether the EB v is charging during its l^{th} break in bus depot $d(l)$ at time interval t.

$$x_{v,l,d(l),t} = \begin{cases} 1, & \text{if the EB } v \text{ is charging during its } l^{th} \text{ break} \\ & \text{in bus depot } d(l) \text{ at time interval } t \\ 0, & \text{otherwise} \end{cases} \tag{4}$$

Here, $d(l)$ represents the depot associated with the l^{th} break of an EB.

Moreover, let the continuous variables $p_{v,l}$ represent the charging power of the EB v during its l^{th} break. Thereby, Equation (5) can be employed to calculate the electricity charged for the EB v during its l^{th} break.

$$q_{v,l} = p_{v,l} \sum_{t \in T} x_{v,l,d(l),t}, \forall v \in V, \forall l \in L_v \tag{5}$$

Constraint (6) guarantees that the charging power of an EB does not surpass the maximum allowable charging power of charging piles.

$$p_{v,l} \le P_{max}, \forall v \in V, \forall l \in L_v \tag{6}$$

Where, P_{max} denotes the charging piles' maximum allowable charging power.

Let SoC_{min} represent the minimum allowable battery SoC for EBs. In this context, SoC refers to the ratio of the current battery charge level to its full capacity, typically expressed as a percentage. Let E_v represent the battery capacity of EB v. Constraints (7) and (8) are formulated to confine the SoC of an EB within a reasonable operational range. Constraint (9) ensures that an EB's SoC must reach 100 % before initiating a schedule. Simultaneously, Constraint (10) ensures that an EB is fully charged after completing all its scheduled trips.

$$E_{v,l} \ge SoC_{min} E_v, \forall v \in V, \forall l \in L_v \tag{7}$$

$$E_{v,l} \le E_v, \forall v \in V, \forall l \in L_v \tag{8}$$

$$E'_{v,0} = E_v, \forall v \in V \tag{9}$$

$$E'_{v,|L_v|} = E_v, \forall v \in V \tag{10}$$

Let $n_j(t)$ denote the number of available charging piles for EBs in bus depot j at time interval t. Constraint (11) ensures that the total number of EBs being charged does not surpass the number of available charging piles allocated to EBs in bus depot j at time interval t.

$$\sum_{v \in V} \sum_{l \in L_v : d(l) = j} x_{v,l,d(l),t} \le n_j(t), \forall j \in J, \forall t \in T \tag{11}$$

As a component of the objective function, the electricity consumed by EBs in bus depot j at time interval t, denoted by $Q^{EB}_{j,t}$, can be calculated as follows.

$$Q^{EB}_{j,t} = \sum_{v \in V} \sum_{l \in L_v : d(l) = j} p_{v,l} x_{v,l,d(l),t}, \forall j \in J, \forall t \in T \tag{12}$$

(2) Facilities in bus depots

Constraint (13) ensures that the allocation of charging piles to EBs and PEVs in bus depot j at any time does not surpass the available number of charging piles deployed in bus depot j.

$$n_j(t) + s_j(t) \le N_j, \forall j \in J, \forall t \in T \tag{13}$$

Here, N_j represents the total number of available charging piles in bus depot j.

Inequality (14) represents a constraint on the energy consumption of solar PV systems in bus depot j at time interval t, ensuring that it does not exceed the minimum of two quantities: $Q_{j,t}$ and $Q^{PV}_{j,t}$.

$$u_{j,t} \le min\left\{ Q_{j,t}, Q^{PV}_{j,t} \right\}, \forall j \in J, \forall t \in T \tag{14}$$

Where, $Q^{PV}_{j,t}$ represents the solar PV energy generated in bus depot j at time interval t, while $Q_{j,t}$ denotes the total electricity consumption in bus

Table 1
Notation of sets, indices, parameters, and variables in the mathematical model.

Notation	Definition
Sets:	
J	Set of bus depots
T	Set of time intervals
V	Set of EBs
L_v	Set of breaks for EB v, $v \in V$
Indices:	
j	Index of bus depots, $j \in J$
t	Index of time intervals, $t \in T$
v	Index of EBs $v \in V$
l	Index of break of EB v, $l \in L_v$
Parameters:	
c_t	Electricity price at time interval t, USD/kWh
c_{emis}	Cost of carbon emissions associated with consuming one kWh of electricity from the grid, USD/kWh
c_{PV}	Equivalent daily cost of installing and operating solar PV systems, USD/kW
Δt	Duration of a single time interval, 1 min
$e_{v,l}$	Accumulated electricity consumed by EB v in the trip before the l^{th} break, kWh
$d(l)$	Bus depot associated with the l^{th} break of EB v
E_v	Battery capacity of EB v, kWh
P_{max}	Maximum allowable charging power of charging piles, kW
SoC_{min}	Minimum SoC allowed for EBs
N_j	Total number of available charging piles in bus depot j
p^{PEV}	Average charging power for PEVs, kW
$\lambda_j(t)$	Poisson arrival rate of PEVs in bus depot j at time interval t, vehicle/minute
$1/\mu$	The mean of the exponentially distributed random charging time for each arriving PEV, minute
$Q_{j,t}^{PV}$	Solar PV energy yield in bus depot j at time interval t, kWh
Variables:	
$E_{v,l}$	Remaining battery electricity of EB v when it is at the beginning of the l^{th} break, kWh
$E'_{v,l}$	Remaining battery electricity of EB v when it is at the end of the l^{th} break, kWh
$x_{v,l,d(l),t}$	$= 1$ if EB v is charging during its l^{th} break in bus depot $d(l)$ at time interval t; $= 0$ otherwise
$p_{v,l}$	Charging power of EB v during the l^{th} break, kW
$q_{v,l}$	Electricity charged for EB v during the l^{th} break, kWh
$Q_{j,t}^{EB}$	Total electricity consumption of EBs in bus depot j at time interval t, kWh
$Q_{j,t}^{PEV}$	Total electricity consumption of PEVsin bus depot j at time interval t, kWh
$Q_{j,t}$	Total electricity consumption in bus depot j at time interval t, kWh
$u_{j,t}$	Energy consumption of solar PV systems in bus depot j at time interval t, kWh
$n_j(t)$	Number of available charging piles for EBs in bus depot j at time interval t
$s_j(t)$	Number of available charging piles for PEVs in bus depot j at time interval t
$N_j(t)$	Number of PEVs being charged in bus depot j at time interval t
$P\{N_j(t) = n\}$	Probability of n PEVs being charged in bus depot j at time interval t
$E[N_j(t)]$	Average number of PEVs being charged in bus depot j at time interval t
$a_j(t)$	Offered load of the queue system in bus depot j at time interval t
$B_j(t)$	Block probability of the queue system in bus depot j at time interval t

depot j at time interval t. This can be calculated using Equation (15).

$$Q_{j,t} = Q_{j,t}^{EB} + Q_{j,t}^{PEV}, \forall j \in J, \forall t \in T \tag{15}$$

3.2.4. Loss queue model for PEV charging demand

In this section, we analyze the charging demand of PEVs arriving in bus depots. This demand depends on the time-dependent arrival rate of PEVs, as well as the capacity and SoC of their batteries. Furthermore, it is crucial to account for the limited number of charging piles available at the bus depot. If a PEV driver arrives and finds no available charging piles, they will leave the depot without recharging. Given these characteristics, this system exhibits similarities to an Erlang B (loss queue) model, which conforms to the $M/M/s/s$ queue theory. This model has been extensively utilized in modeling electric vehicle charging demand [37,38]. Specifically, the first M in $M/M/s/s$ denotes that PEVs arrive at a bus depot following a Poisson distribution. The second M indicates that the service (charging) duration for each PEV follows an exponential distribution. The third s signifies that there are s identical charging piles available, allowing s PEVs to charge in parallel at the bus depot. The final s indicates that the capacity of the bus depot for PEVs is limited to s, implying no waiting areas for PEVs. To evaluate this loss queuing system, the primary metric is termed as the block probability, which quantifies the probability that a PEV driver arriving at the depot finds no available charging piles.

Let $B_j(t)$ denote the block probability of the queue system in bus depot j at time interval t, as defined by Equation (16). It is noteworthy that this equation is derived from the property of independent increments in the Poisson process.

$$B_j(t) = P\{N_j(t) = s_j(t) | \text{an arrival occurs in } (t, t+dt)\} = P\{N_j(t) = s_j(t)\}, \quad \forall j \in J, \forall t \in T \tag{16}$$

Where $N_j(t)$ represents the number of PEVs being charged in bus depot j at time interval t, and $s_j(t)$ indicates the number of available charging piles for PEVs in bus depot j at time interval t.

The expected number of PEVs being charged in bus depot j at time t, denoted by $E[N_j(t)]$, can be expressed by the following differential equation. This equation represents the difference between the effective arrival rate and the service rate of PEVs in bus depot j at time interval t.

$$\frac{d}{dt}E[N_j(t)] = \lambda_j(t)(1 - B_j(t)) - (\mu P\{N_j(t) = 1\} + 2\mu P\{N_j(t) = 2\} + \ldots + s_j(t)\mu P\{N_j(t) = s_j(t)\}), \forall j \in J, \forall t \in T \tag{17}$$

Here, $\lambda_j(t)$ and μ denote the time-dependent arrival and service rates of PEVs in bus depot j at time interval t, respectively. Evidently, the above Equation (17) can be reformulated into the following expression for simplification.

$$\frac{d}{dt}E\left[N_j(t)\right]=\lambda_j(t)\left(1-B_j(t)\right)-\mu E\left[N_j(t)\right],\forall j\in J,\forall t\in T \tag{18}$$

Since the above differential equation involves two unknown variables, $E\left[N_j(t)\right]$ and $B_j(t)$, an additional equation relating these two variables is necessary for solving it. Notably, the time-dependent expected number of PEVs being charged at the depot $E\left[N_j(t)\right]$ can be formulated in terms of the time-dependent block probability $B_j(t)$ and the offered load $a_j(t)$ as follows.

$$E\left[N_j(t)\right]=\left(1-B_j(t)\right)a_j(t),\forall j\in J,\forall t\in T \tag{19}$$

Because the PEV arrival rate varies over time, it results in a nonstationary loss queue [39]. Therefore, it is not applicable to directly calculate the time-dependent offered load using $a_j(t)=\lambda_j(t)/\mu$, as this method is specific to stationary queue systems. Consequently, the time-dependent offered load $a_j(t)$ remains unknown, necessitating the incorporation of an additional complementary equation. Drawing inspiration from Alnowibet and Perros [40], Equation (19) can be rearranged to express the time-dependent offered load $a_j(t)$ as follows.

$$a_j(t)=\frac{E\left[N_j(t)\right]}{1-B_j(t)},\forall j\in J,\forall t\in T \tag{20}$$

After reasonably expressing the time-dependent offered load $a_j(t)$ in terms of $E\left[N_j(t)\right]$ and $B_j(t)$, the well-known Erlang B formula appears to be a suitable complementary equation as follows.

$$B_j(t)=\frac{\left[a_j(t)\right]^{s_j(t)}/s_j(t)!}{\sum_{s=0}^{s_j(t)}\left(\left[a_j(t)\right]^{s}/s_j(t)!\right)},\forall j\in J,\forall t\in T \tag{21}$$

Although Equation (21) is dependent on $a_i(t)$ in stationary steady-state queue systems, it has served as a complementary equation in some effective numerical methods for approximating the time-dependent block probability [40,41]. Moreover, this equation can be shown to be exact when there is only one available charging pile, i.e., $s_j(t)=1$. Readers interested in the proof can refer to the Appendix A. Therefore, the expected number of PEVs being charged at any depot at any time can be determined by solving the set of equations comprising Equations (18), (20), and (21). To solve this set of equations efficiently, we developed a numerical approach combining Euler's method and fixed-point iteration method, as shown in Appendix B.

Finally, as a component of the objective function, the electricity consumed by PEVs in bus depot j at time interval t, denoted by $Q_{j,t}^{PEV}$, can be calculated as follows.

$$Q_{j,t}^{PEV}=E\left[N_j(t)\right]p^{PEV}\Delta t,\forall j\in J,\forall t\in T \tag{22}$$

Here, p^{PEV} represents the average charging power for PEVs, and Δt denotes the duration of a single time interval.

3.3. Summary of the mathematical model

The proposed model, detailed in Section 3.2, is optimized using objective function (1) and is subject to constraints (2) through (22). Specifically, Equation (5) involves the product of variables, resulting in a nonlinear formulation that complicates the direct solution. To address this, we linearized Equation (5) using a standard technique (see Appendix C), transforming the optimization problem into a MILP that can be efficiently solved by commercial solvers such as Gurobi.

4. Numerical experiments

4.1. Real-world case study

To validate the effectiveness of our proposed model, we conducted a case study focusing on EBs and PEVs charging at shared bus depots in Beijing's downtown area. Our study began with the acquisition of a multi-source dataset comprising GPS trajectory data from 396 EBs across 24 bus routes, along with temperature and irradiance data. Additionally, we gathered charging data from 12,603 PEVs over a one-week period within a 2-km radius of these bus depots. This rich dataset enabled us to model the time-dependent arrival rates and average electricity consumption associated with PEV charging demands at these shared bus depots.

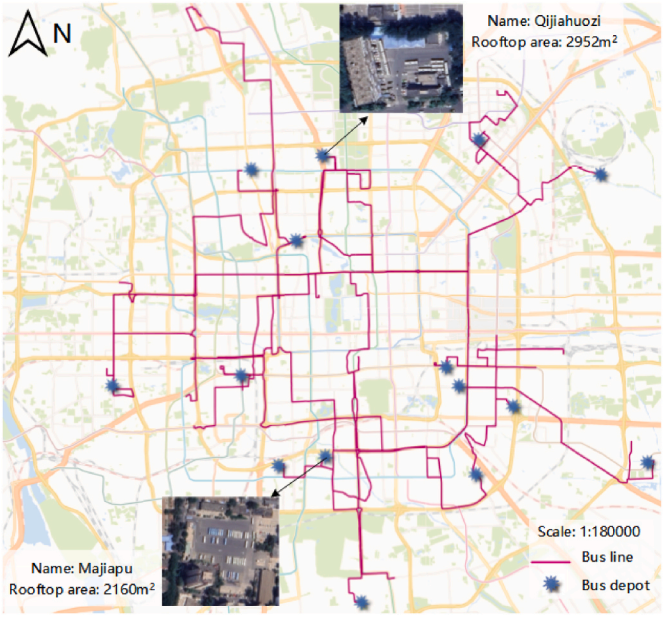

Fig. 2. The investigated bus network in Beijing.

All programs were implemented in Python and executed on an Intel Core i7-11700 CPU (2.50 GHz) with 16 GB of RAM. Gurobi version 10.0.3 was employed to perform the experiments. To balance precision with computational efficiency, the control time interval for the EB and PEV sectors was set to 2 min, while the control time interval for facilities in bus depots was set to 60 min. The simulation time horizon spans a full day, with solution times consistently less than 1 s for all cases studied.

4.1.1. Description of bus operational data

We collected bus trajectory data at time steps of 5–10 s on October 19, 2020. It includes key elements such as bus ID, GPS timestamps, coordinates, and speed. We also gathered vehicle information data containing key elements such as mass, length, height, and battery capacity of EBs. Both bus trajectory data and vehicle information data use the same bus ID field to ensure precise identification of different EBs' spatiotemporal activity patterns. Furthermore, we calculated the depot-specific rooftop area suitable for PV panel installations through built environment data. Fig. 2 illustrates the bus network used in this case study.

4.1.2. Parameter setting

We adopted the longitudinal dynamics model outlined by Gallet, Massier and Hamacher [42] to estimate the electricity consumption for each trip in the EB schedules. Regarding the parameters in the objective function, electricity prices are based on Beijing's time-of-use tariffs shown in Fig. 3. The cost of carbon emissions (c_{emis}) associated with consuming one kWh of electricity from the grid is determined to be 0.0088 USD/kWh according to Liu, Yeh, Plötz, Ma, Li and Ma [43]. Additionally, the equivalent daily cost of installing and operating solar PV systems (c_{PV}) is defined as 0.07 USD/kW, referring to Liu, Yeh, Plötz, Ma, Li and Ma [43]. For other parameters, the maximum allowable charging power (P_{max}) for our study is limited to 100 kW. This power constrains the average charging power throughout the entire charging

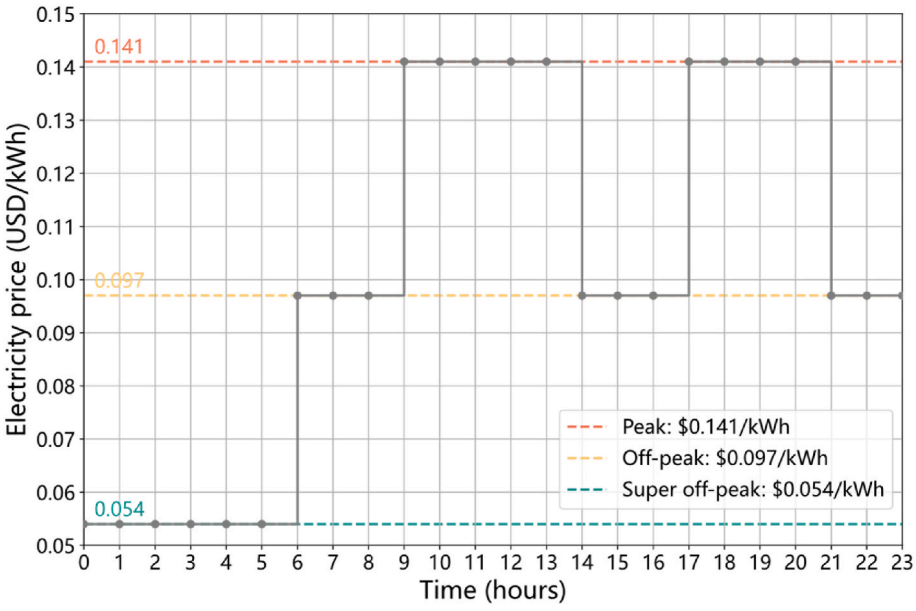

Fig. 3. Time-of-use tariffs in Beijing.

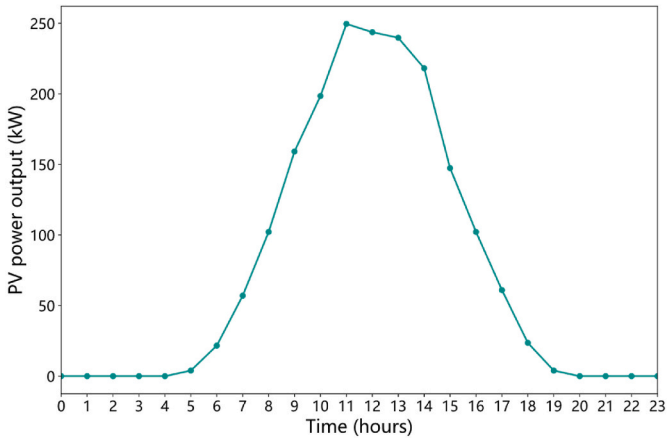

Fig. 4. Average time-dependent solar PV output of the Majiapu depot in June.

process of EBs. The average charging power for PEVs (p^{PEV}) is set to 30 kW. Furthermore, the minimum SoC (SoC_{min}) for EBs is fixed at 20 %. The number of available charging piles in each bus depot is consistent with reality based on empirical data.

4.1.3. Temperature and irradiance data

In our case study, the temperature and irradiance data, encompassing both beam and diffuse irradiance, were collected hourly every day in 2020. We employed the empirical equations from Chandra Mouli, Bauer and Zeman [44] along with the collected data to compute the depot-specific power output of solar PV systems. The computed results of solar PV power outputs at different hours for the Majiapu depot in June are shown in Fig. 4.

4.1.4. PEVs data

The collected PEV charging data includes charging location, charging start time, charging end time, and time-specific charged electricity. This data allows us to calculate the average time-dependent arrival rate and average electricity consumption of PEVs based on charging demand. Fig. 5 illustrates the time-dependent charging demand of PEVs around the Majiapu depot.

4.2. Results

4.2.1. Economic and environmental benefits of solar PV and the shared charging mode

We compared our proposed shared charging strategy with two benchmark operational strategies to assess the economic and environmental benefits of solar PV and the shared charging mode in the case study. The first benchmark is an operational strategy incorporating solar PV but not sharing the charging piles with PEVs. The second benchmark is an operational strategy that neither incorporates solar PV nor shares the charging facilities with PEVs. We used the total cost, EB charging cost, CO_2 emissions cost, solar PV cost, and savings in charging cost to assess the performance of the operational strategies. Fig. 6 shows the performance comparison results of different operational strategies.

For the sake of comparison, we use "PVPEVs" to denote the operational strategy incorporating solar PV and the shared charging mode, "PV" to indicate the operational strategy incorporating solar PV without the shared charging mode, and "BS" to denote the baseline operational strategy without solar PV nor the shared charging mode.

According to Fig. 6, although PVPEVs and PV have additional upfront and operational solar PV costs in the deployment area compared to BS, they can save 22.05 % and 8.48 % of the total cost, respectively. This indicates that solar PV deployment offers significant economic benefits. The greatest economic benefits of solar PV arise from savings in charging costs, with PVPEVs and PV saving 64.62 % and 52.84 %, respectively. Regarding environmental benefits, PVPEVs and PV can reduce CO_2 emissions costs by 35.61 % and 30.07 %, respectively. Notably, an interesting finding is that both PVPEVs and PV incur higher EB charging costs compared to BS. To further investigate this, Fig. 7 illustrates the EB charging demand for two bus depots under three operational strategies. It is observed that EB charging demand shifts from nighttime to daytime hours to utilize solar PV output but incurs charges at peak electricity prices in the PVPEVs and PV approaches. Conversely, in the BS approach, EBs primarily complete charging at night when electricity prices are lowest.

To evaluate the economic and environmental benefits of the shared charging mode, we compared the results of PVPEVs and PV in Fig. 6 (a) and 6 (b). The comparison shows that sharing the charging piles with PEVs can reduce CO_2 emissions costs by 7.93 % and save 27.86 % on charging costs. This indicates that introducing the shared charging mode can improve solar energy on-site consumption, thereby improving the

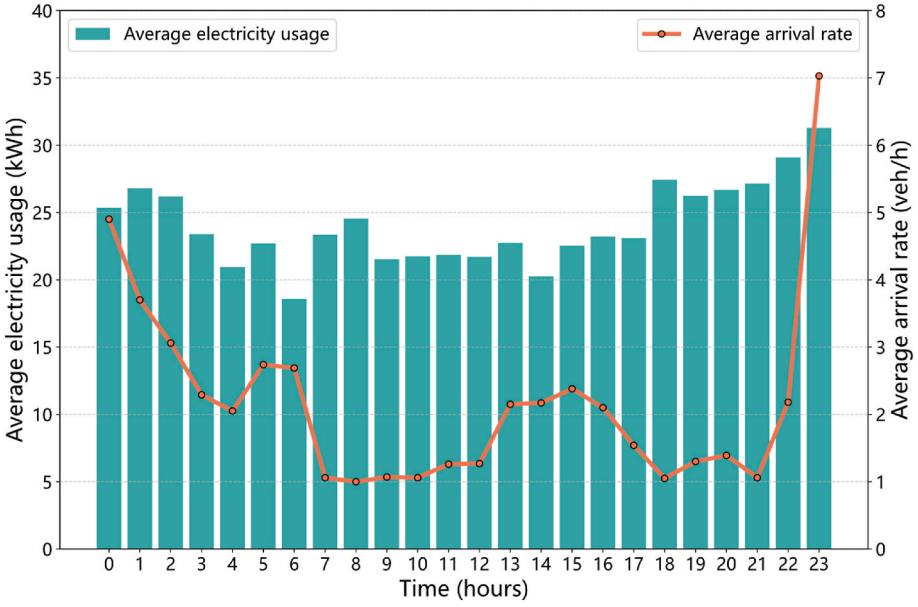

Fig. 5. Average time-dependent arrival rate and electricity consumption of PEV charging demand in June.

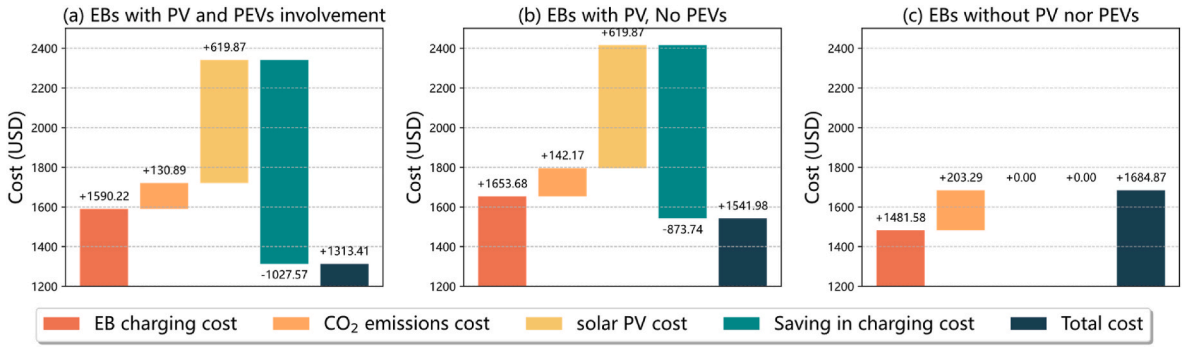

Fig. 6. Economic analysis of solar PV and the shared charging mode.

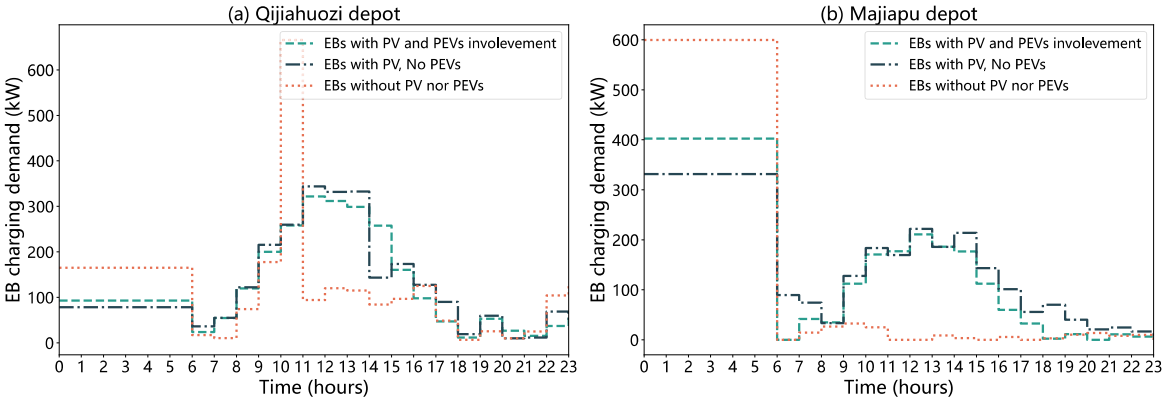

Fig. 7. EB charging demand in different operational strategies at two bus depots in June.

benefits of solar PV. We analyze this in detail in the next section.

4.2.2. *Impact of PEVs on solar energy on-site consumption*

Fig. 7 illustrates the charging demand distributions of EBs at two bus depots for PVPEVs, PV, and BS. This section primarily focuses on comparing PVPEVs and PV. The results reveal that PVPEVs exhibit a higher charging demand than PV at night when electricity prices are lowest. Conversely, during the daytime, when solar PV output is available, PVPEVs show a lower charging demand compared to PV. This occurs because PEVs can utilize solar PV output during the daytime under the shared charging mode, allowing some EBs to charge at night when electricity prices are lowest.

To investigate the improvement in solar PV utilization by PVPEVs, we compared the solar PV usage between PVPEVs and PV at two depots,

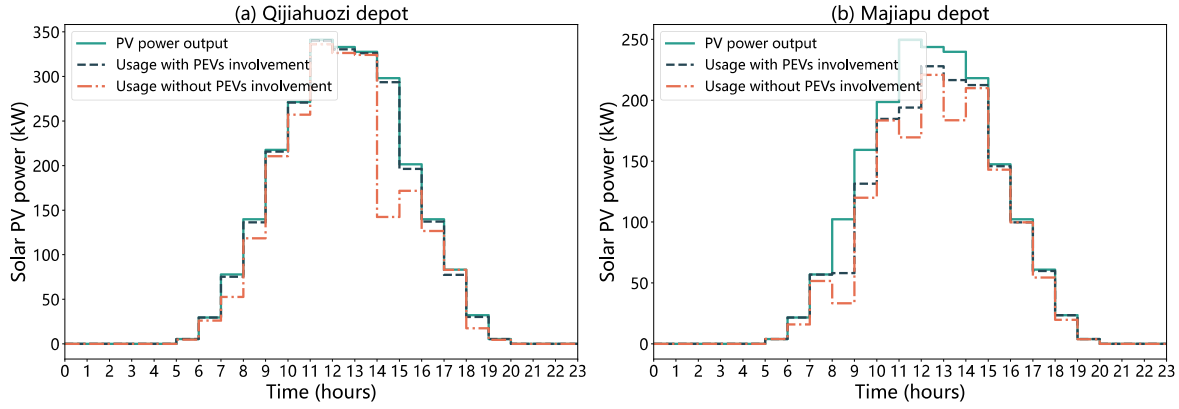

Fig. 8. Solar PV output power and usage power in different operational strategies at two depots in June.

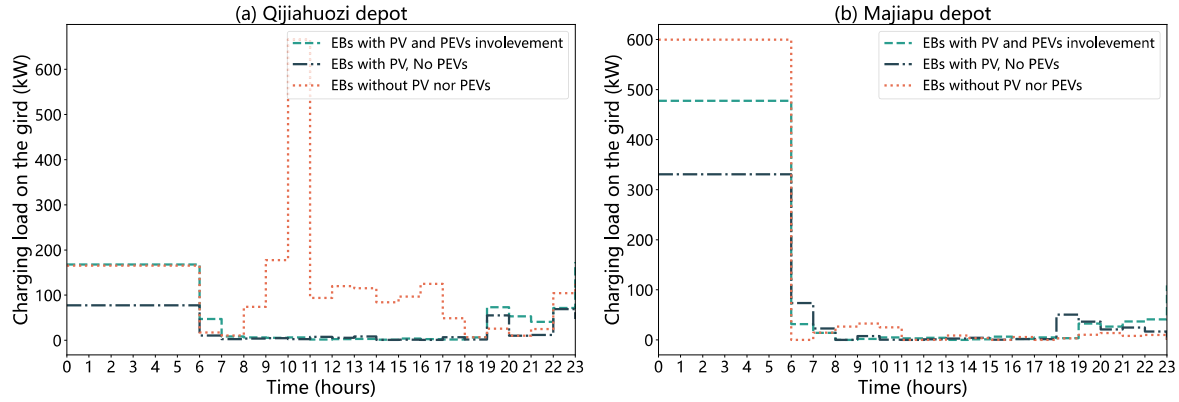

Fig. 9. Charging load on the gird in different operational strategies at two bus depots in June.

as shown in Fig. 8. The results reveal that the solar PV usage distribution for PVPEVs is closer to the solar PV output compared to PV. Furthermore, the total solar PV utilization rate of 15 depots for PVPEVs and PV is 92.91 % and 79.30 %, respectively. Notably, as shown in Fig. 7 and 8, an interesting finding is that although PVPEVs have lower EB charging demand during the daytime compared to PV, they achieve higher solar PV utilization. This is because PEV charging demand is transformed into additional consumption of solar PV output during the daytime, thereby

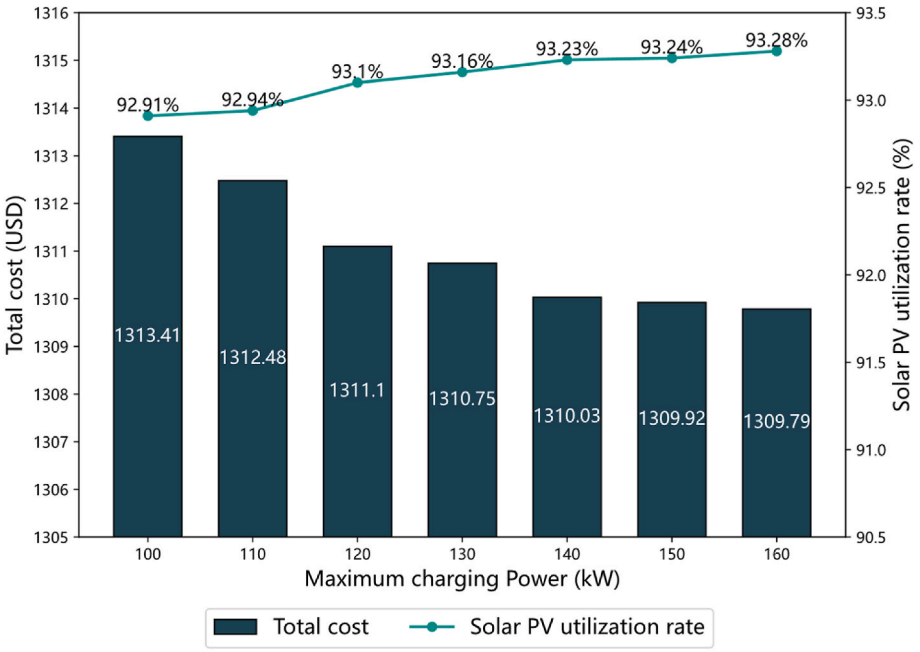

Fig. 10. Impact of different maximum allowable charging power on solar PV utilization and overall daily system costs.

compensating for the limited consumption capacity of EBs. Consequently, sharing the charging piles with PEVs improves the solar energy on-site consumption.

4.2.3. Impact of PEVs on gird loads

In this section, we analyzed the influence of the shared charging mode on the grid load. Fig. 9 shows the charging load on the grid in two depots for PVPEVs, PV, and BS, revealing that PVPEVs and PVs have a lower charging load on the grid compared to BS. Specifically, the daily reduction in the total charging load of 15 bus depots on the grid for PVPEVs was 29.55 % and 55.62 %, respectively, compared to BS. We further analyzed the total charging load of 15 bus depots on the grid at different periods with different electricity prices. During periods of peak electricity prices, the total charging load on the grid for PVPEVs and PVs decreased by 82.61 % and 83.56 %, respectively, compared to BS. During periods of off-peak electricity prices, the total charging load on the grid for PVPEVs and PVs decreased by 18.08 % and 60.04 %, respectively, compared to BS. Furthermore, during periods of super off-peak electricity prices, the total charging load on the grid for PVPEVs and PV decreased by 15.68 % and 46.66 %, respectively, compared to BS. Notably, although introducing the shared charging mode in PVPEVs can reduce the charging load on the grid compared to BS, it leads to an increase in the charging load on the grid compared to PV. The reason for this phenomenon is that the charging demand of PEVs contributes not only to solar PV energy consumption but also to additional charging load. However, PVPEVs and PV have a similar rate of charging load reduction compared to BS during periods of peak electricity prices. Therefore, although the shared charging mode leads to a higher charging load compared to PV due to the shared charging facilities with PEVs, the additional charging load almost always occurs during off-peak periods of the grid, which has a less negative impact on the grid. In summary, these findings provide insight into how the shared charging mode can improve solar PV utilization and reduce overall system daily costs without negatively impacting the grid load during peak periods.

4.3. Sensitivity analysis

4.3.1. Maximum allowable charging power

The impact of different maximum allowable charging power on solar PV utilization and overall daily system costs was investigated by increasing the maximum allowable charging power from 100 kW to 160 kW in 10 kW increments. Fig. 10 illustrates how increasing the maximum allowable charging power impacts total costs and solar PV utilization. We found that total costs decrease and PV utilization increases with higher maximum allowable charging power. However, relative to a baseline of 100 kW, the maximum decrease in total cost is 0.28 %, and the maximum increase in solar PV utilization is 0.40 % over this range of charging power adjustments. Moreover, when the maximum allowable charging power exceeds 150 kW, additional increases do not significantly impact total costs or solar PV utilization. These results suggest that the total cost of the system and solar PV utilization under our proposed operational strategy are resilient to changes in maximum allowable charging power.

4.3.2. Charging service fee for electric vehicles

In our proposed operational strategy, no fees are charged to PEV owners for charging services. In this section, we examine the impact of changes in charging service prices on various cost components and solar PV utilization. We gradually increase the service price during peak periods in small increments (0.01USD/kWh), ranging from 0 to 0.05USD/kWh, and simultaneously increase the service price during off-peak periods by 0.005USD/kWh, ranging from 0 to 0.025USD/kWh. According to Fig. 11, the various cost components, except for charging service revenue, are not sensitive to the changes in charging service prices. Moreover, the results indicate that the increased charging service prices result in an overall reduction in total cost. However, when service fees are charged to PEV owners, the EB charging cost and the CO_2 emissions cost increase while the savings in charging costs decrease. As Fig. 12 shows, more charging piles are allocated to PEVs, thereby reducing the available charging piles for EBs. This implies that some EBs cannot charge at the optimal time when electricity prices are low, thereby increasing the EB charging cost. Additionally, the decrease in

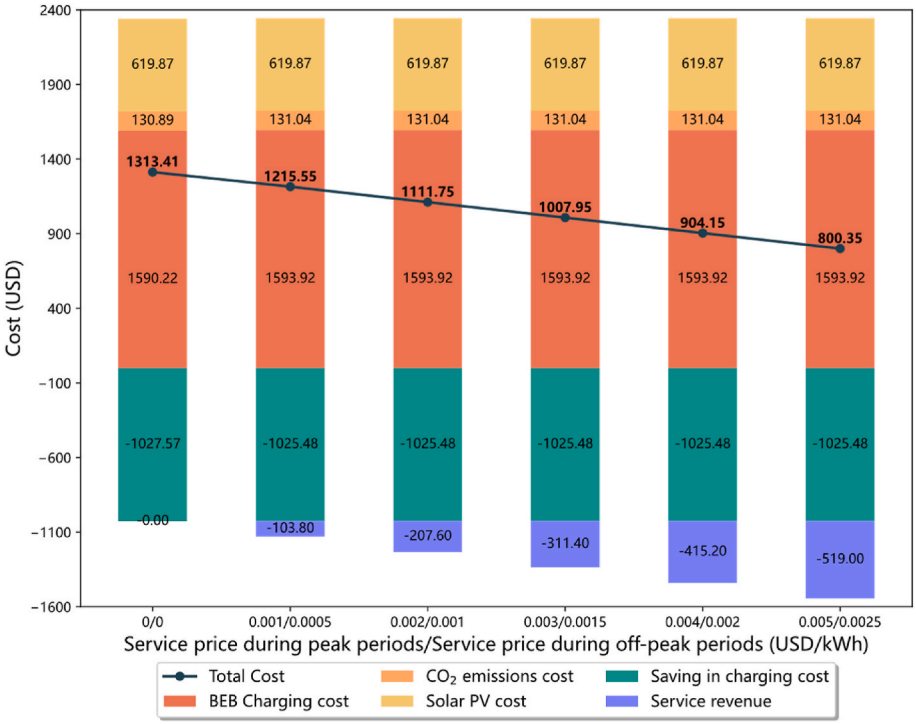

Fig. 11. Impact of Charging service fee for electric vehicles on daily system costs.

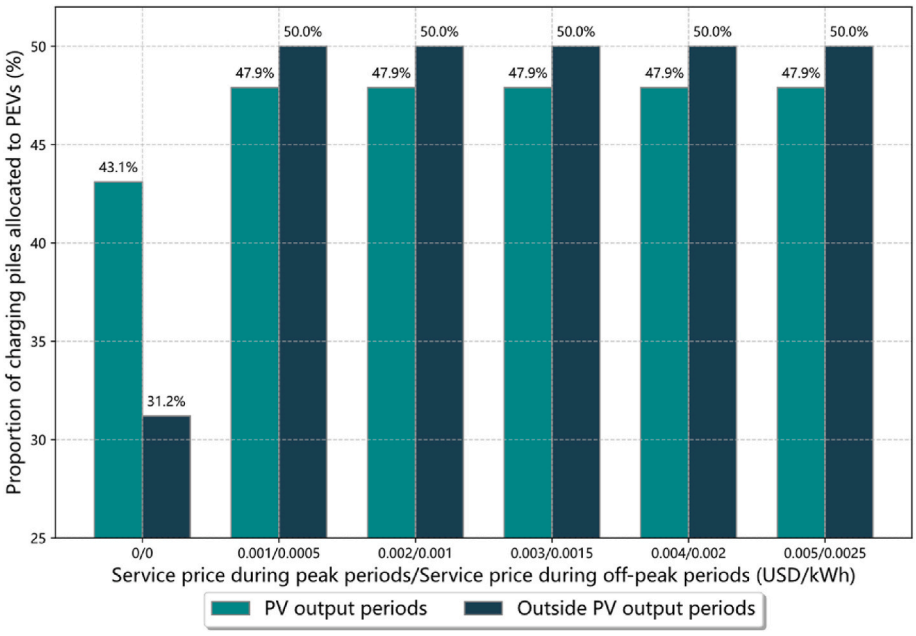

Fig. 12. Impact of Charging service fee for electric vehicles on the proportion of charging piles allocated to PEVs.

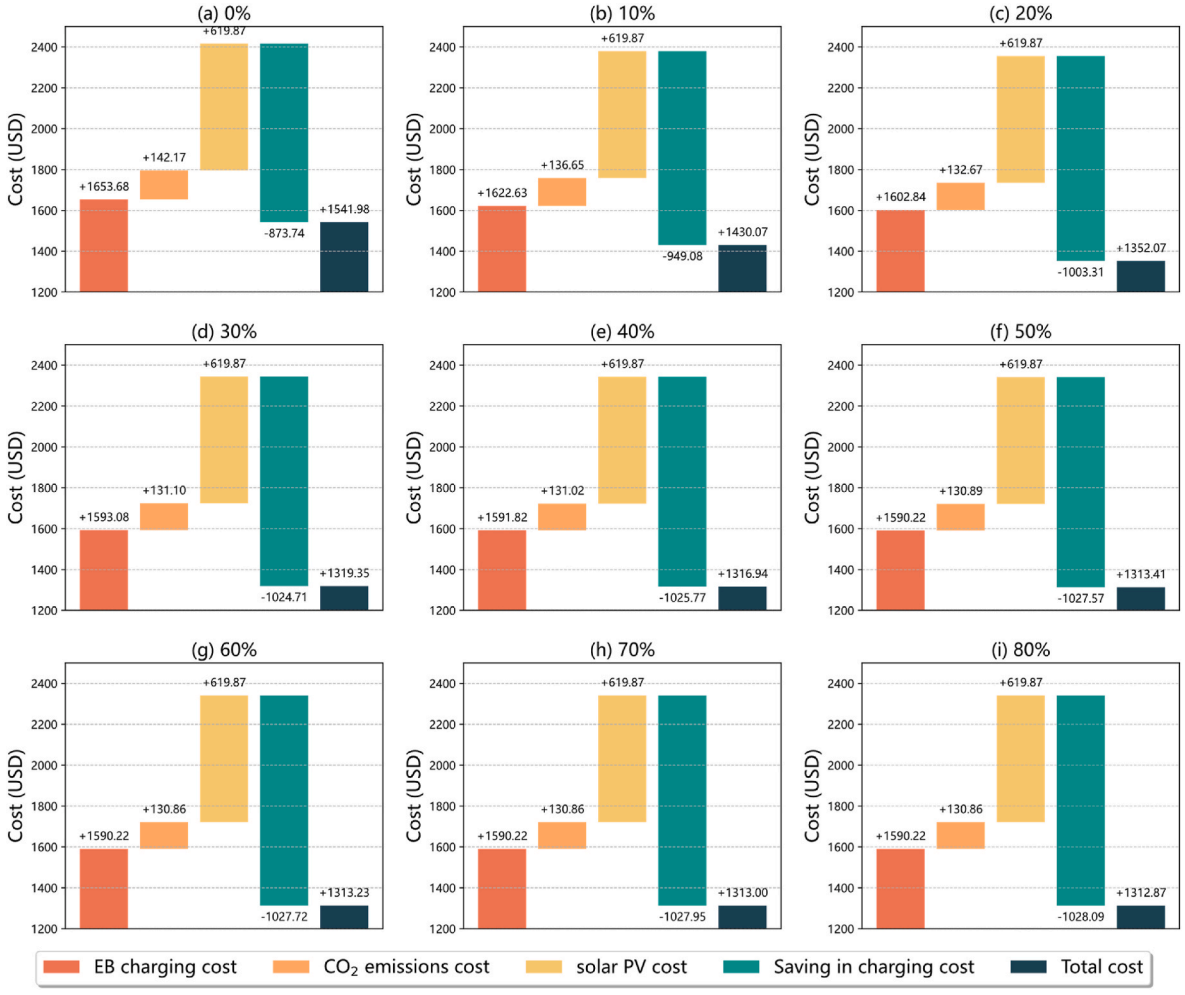

Fig. 13. Impact of limited number of charging piles available for PEVs on daily system costs.

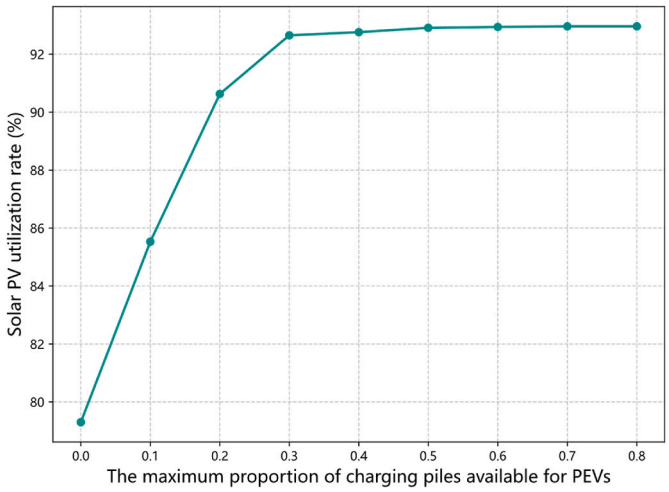

Fig. 14. Impact of limited number of charging piles available for PEVs on solar PV utilization.

revenue from savings in charging costs and the increase in CO_2 emissions cost directly indicate a decrease in solar PV utilization. In summary, these observations suggest that, although charging service fees can directly generate profit, they can lead to a decrease in solar PV efficiency.

4.3.3. *Limited number of charging piles available for PEVs*

In our proposed operational strategy, the maximum proportion of charging piles available for PEVs is set at 50 %. This section investigates the impact of varying this proportion on cost components and solar PV utilization. We incrementally increased the proportion from 0 to 0.8 in steps of 0.1. As shown in Fig. 13, all cost components, except solar PV costs, decrease significantly as the proportion increases from 0 to 0.5. Beyond the 50 % threshold, the sensitivity of cost components to further increases diminishes. Similarly, as shown in Fig. 14, solar PV utilization rises but plateaus once the proportion reaches 0.5. These results suggest that there is limited benefit in allocating more than 50 % of the charging piles to PEVs.

4.3.4. *Weather conditions*

In our operational strategy, we use June's average solar PV output to represent typical weather conditions. This section examines how weather variability impacts overall daily system costs and solar PV utilization. As shown in Fig. 15, the trends over the year indicate that solar PV utilization remains consistently high, despite a notable dip in April. Interestingly, April also shows the lowest system costs, likely due to excess PV output that the system is unable to fully utilize. In contrast, months such as January, February, November, and December experience higher utilization but come with increased system costs, reflecting reduced financial benefits for operators during these periods. These findings reveal that weather conditions directly impact solar PV output and, consequently, daily system costs. However, even during challenging months like January, the system with solar PV still outperforms a system without PV integration, suggesting that the region's charging depots offer strong potential for solar PV adoption.

5. Discussion

This study develops an optimization model that integrates shared charging services for PEVs within bus depots equipped with solar PV systems, aiming to maximize on-site solar energy utilization. The model specifically addresses the operational phase of urban PT systems, where the configuration of charging depots, including the number of solar panels and charging piles, is predefined. It optimizes EB charging schedules and allows PEVs to use idle charging piles during periods of peak solar energy generation. This dual usage improves energy efficiency and reduces dependency on grid electricity, particularly during peak hours.

Although the model assumes flexibility in charging power, implementing this may require technical upgrades to both vehicles and infrastructure. The model can also be adapted to scenarios with fixed charging power to ensure reliability across different operational conditions.

For PT operators and government decision-makers, this model provides key insights into optimizing daily charging schedules for both EBs and PEVs in response to varying charging demands and solar energy availability. The results highlight the substantial potential for cost savings and CO_2 emission reductions, making this model a vital tool for enhancing the sustainability of urban PT systems. In our case study, shared charging services increased solar PV utilization from 79.30 % to 92.91 %, reduced daily system costs by 14.82 %, and lowered CO_2 emissions by 7.93 %. Nonetheless, sensitivity analysis underscores the need for careful management to prevent shared charging from

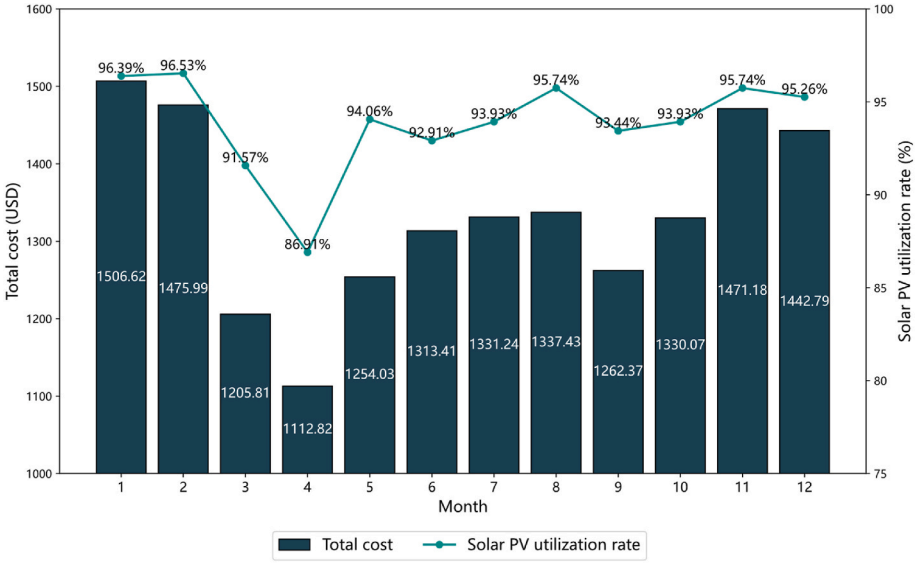

Fig. 15. Impact of weather condition on overall daily system costs and solar PV utilization.

diminishing solar PV efficiency, despite potential profits from PEV service fees.

6. Conclusion

This study explores the potential of sharing charging piles with PEVs in bus depots equipped with solar PV systems to improve solar energy on-site consumption and reduce the overall daily system cost. This shared charging mode allows PEVs to use charging piles in bus depots, which are idle during the daytime. Specifically, a mixed-integer linear programming model is formulated to jointly optimize the EB charging scheduling and the allocation of charging facilities between EBs and PEVs throughout the day. Meanwhile, the stochastic nature of PEV charging demand is modeled as a loss queue model with time-dependent arrival rates. A case study is conducted on a bus network in Beijing, involving 15 bus depots and 24 routes, to validate the effectiveness of sharing charging mode through a comparison analysis with two operational strategies without solar PV systems. This evaluation leverages multi-source data such as operational data of EBs, charging demand data of PEVs, and temperature and irradiance data. The findings demonstrate that integrating shared charging in bus depots equipped with solar PV systems improves solar PV utilization from 79.30 % to 92.91 %. This integration leads to reductions in CO_2 emissions costs and overall daily system costs by 7.93 % and 14.82 %, respectively, without negatively impacting the grid load during peak periods. In-depth analysis reveals that performance improvements are achieved by sharing charging piles with PEVs to consume solar PV energy during the daytime, thus eliminating the need for some EBs to shift their charging demand from nighttime to daytime hours with abundant solar PV energy. Moreover, sensitivity analysis shows that although charging service fees to PEVs can directly generate profit, they can lead to a decrease in solar PV efficiency. The results further indicate that there is no significant difference in various cost components as the maximum allowable charging power varies within a higher range. This finding is consistent with the conclusions of Liu, Yeh, Plötz, Ma, Li and Ma [43].

In this study, we conducted an initial evaluation of the economic and environmental benefits of the shared charging mode. Through offline optimization, we provided daily operation schedules and charging pile allocation plans for public transport operators. However, given the significant variability in passenger demand throughout the day [45,46], real-time adjustments to bus timetables and departure schedules are often required. Addressing the control of charging schedules and resource allocation in such dynamic conditions is critical. The development of online control algorithms, such as machine learning and AI-based methods, represents a promising avenue for future research [47–49]. Additionally, while the Erlang B model used here provides a useful simplification, it does not fully capture the dynamic decision-making behaviors of individual PEV drivers, such as their preferences for charging services based on factors like accessibility, price, or speed. The introduction of new shared charging services could also influence PEV driver behavior in ways not fully accounted for in this model. This simplification is acknowledged as a limitation in addressing dynamic scheduling problems, and future research could explore models that incorporate these behavioral factors.

CRediT authorship contribution statement

Zhengke Liu: Writing – original draft, Methodology, Investigation, Conceptualization. **Xiaolei Ma:** Writing – review & editing, Supervision, Resources, Funding acquisition, Formal analysis. **Siyu Zhuo:** Writing – review & editing, Visualization, Software, Investigation. **Xiaohan Liu:** Writing – review & editing, Validation, Supervision, Methodology, Investigation.

Declaration of competing interest

The authors declare that they have no known competing financial interests or personal relationships that could have appeared to influence the work reported in this paper.

Acknowledgement

This paper is supported by National Key R&D Program of China (2023YFB2604600), Beijing Natural Science Foundation (JQ24051), and Beijing Nova Program (20230484432).

Appendix A. Proof of proposition

Proposition: $B_j(t) = \frac{[a_j(t)]^{s_j(t)}/s_j(t)!}{\sum_{s=0}^{s_j(t)}([a_j(t)]^s/s_j(t)!)}$ is valid when $s_j(t) = 1, \forall j \in J, \forall t \in T$.

Proof:

Let $s_j(t) = 1$. According to the formula for mean calculation, the following equation holds true:

$$E[N_j(t)] = 0 \bullet P\{N_j(t) = 0\} + 1 \bullet P\{N_j(t) = 1\} = P\{N_j(t) = 1\} \tag{A.1}$$

Substituting $s_j(t) = 1$ into Equation (13), We have:

$$B_j(t) = P\{N_j(t) = 1\} \tag{A.2}$$

Therefore, substituting $P\{N_j(t) = 1\} = B_j(t)$ from Equation (A.2) into Equation (A.1), we get:

$$E[N_j(t)] = B_j(t) \tag{A.3}$$

Substituting $E[N_j(t)] = B_j(t)$ from Equation (A.3) into Equation (16), we obtain:

$$B_j(t) = (1 - B_j(t)) \bullet a_j(t) \tag{A.4}$$

From Equation (A.4), we derive:

$$B_j(t) = \frac{a_j(t)}{1 + a_j(t)} = \frac{a_j(t)/1!}{[a_j(t)]^0/0! + [a_j(t)]^1/1!} = \frac{[a_j(t)]^{s_j(t)}/s_j(t)!}{\sum_{s=0}^{s_j(t)}([a_j(t)]^s/s_j(t)!)} \tag{A.5}$$

Therefore, $B_j(t) = \frac{[a_j(t)]^{s_j(t)}/s_j(t)!}{\sum_{s=0}^{s_j(t)}\left([a_j(t)]^s/s_j(t)!\right)}$ holds true when $s_j(t) = 1$. This completes the proof.

Appendix B. Numerical solution for loss queue model

To calculate the expected number of PEVs being charged at any depot at a given time, we need to solve a set of equations, namely Equations (15), (17), and (18), as outlined below:

$$\begin{cases} \dfrac{d}{dt}E[N_j(t)] = \lambda_j(t)\left(1 - B_j(t)\right) - \mu E[N_j(t)] \\ a_j(t) = E[N_j(t)]/1 - B_j(t) \\ B_j(t) = \dfrac{a_j(t)^{s_j(t)}/s_j(t)!}{\sum_{s=0}^{s_j(t)}\left(a_j(t)^s/s!\right)} \end{cases}, \forall j \in J, \forall t \in T \tag{B.1}$$

Given that Equation (15) is a linear differential equation, it can be addressed using numerical methods. In this study, we employed Euler's method due to its computational efficiency. Accordingly, we make the following assumptions:

$$\frac{d}{dt}E[N_j(t)] \approx \frac{\Delta E[N_i^k(t)]}{\Delta t}, \forall j \in J, \forall t \in T \tag{B.2}$$

Where Δt is sufficiently small. Consequently, Equation (15) can be rewritten as follows:

$$\frac{\Delta E[N_i^k(t)]}{\Delta t} = \lambda_j(t)\left(1 - B_j(t)\right) - \mu E[N_j(t)], \forall j \in J, \forall t \in T \tag{B.3}$$

This can be further rearranged to give:

$$E\left[N_j^k(t)\right] - E[N_j(t-\Delta t)] = \lambda_j(t)\left(1 - \widehat{B}_j^k(t)\right)\Delta t - \mu \Delta t E[N_j(t)], \forall j \in J, \forall t \in T \tag{B.4}$$

Simplifying, we get:

$$(1+\mu\Delta t)E\left[N_j^k(t)\right] = E[N_j(t-\Delta t)] + \lambda_j(t)\left(1 - \widehat{B}_j^k(t)\right)\Delta t, \forall j \in J, \forall t \in T \tag{B.5}$$

Finally, solving for $E[N_i^k(t)]$, we obtain:

$$E\left[N_j^k(t)\right] = \left[E[N_j(t-\Delta t)] + \lambda_j(t)\left(1 - \widehat{B}_j^k(t)\right)\Delta t\right] \Big/ (1+\mu\Delta t), \forall j \in J, \forall t \in T \tag{B.6}$$

To efficiently solve the set of equations, we developed a numerical approach that combines Euler's method with the fixed-point iteration method, as detailed in Algorithm 1.

Algorithm 1. Loss queue model with time-dependent arrival rates and servers

Input: time-dependent arrival rate $\lambda_j(t)$, number of available charging piles $s_j(t)$, service rate μ, time interval size Δt.

for $j \in J$ **do**
  Initialize $t = 0$ and $E[N_j(t)] = 0$;
  while $t \le |T|$ **do**
    Set $k = 0$ and $B_j^k(t) = 0$;
    while True **do**
      $E[N_j^k(t)] = \left[E[N_j(t-\Delta t)] + \lambda_j(t)\left(1 - \hat{B}_j^k(t)\right)\Delta t\right]/(1+\mu\Delta t)$;
      $a_j^k(t) = E[\hat{N}_j^k(t)]/\left(1 - \hat{B}_j^k(t)\right)$;
      $B_j^{k+1}(t) = \frac{[\hat{a}_j^k(t)]^{s_j(t)}/s_j(t)!}{\sum_{j=0}^{s_j(t)}\left([\hat{a}_j^k(t)]^s/s_j(t)!\right)}$;
      if $\left\|B_j^{k+1}(t) - B_j^k(t)\right\| < \epsilon$ **then**
        break;
      end if
      Set $k = k + 1$;
    end while
    Set $B_j(t) = B_j^{k+1}(t)$;
    Set $E[N_j(t)] = E[N_j^k(t)]$;
    Set $t = t + \Delta t$;
  end while
end for
return $E[N_j(t)]$ and $B_j(t)$ for $0 \le t \le |T|$ for $j \in J$.

Appendix C. Linearization of nonlinear constraints

In our proposed model, Equation (5) contains the product of an integer variable $p_{v,l}$ and a binary variable $x_{v,l,d(l),t}$ (where $x_{v,l,d(l),t} \in \{0,1\}$) which is nonlinear. To linearize this product, we introduce an auxiliary variable $z_{v,l,d(l),t}$ such that:

$$z_{v,l,d(l),t} = p_{v,l} \bullet x_{v,l,d(l),t}, \forall v \in V, \forall l \in L_v, \forall t \in T \tag{C.1}$$

To achieve the linearization of Equation (C.1), the following constraints are added:

$$z_{v,l,d(l),t} \leq p_{v,l}, \forall v \in V, \forall l \in L_v, \forall t \in T \tag{C.2}$$

$$z_{v,l,d(l),t} \leq x_{v,l,d(l),t}, \forall v \in V, \forall l \in L_v, \forall t \in T \tag{C.3}$$

$$z_{v,l,d(l),t} \geq p_{v,l} - M \bullet \left(1 - x_{v,l,d(l),t}\right), \forall v \in V, \forall l \in L_v, \forall t \in T \tag{C.4}$$

$$z_{v,l,d(l),t} \geq 0, \forall v \in V, \forall l \in L_v, \forall t \in T \tag{C.5}$$

Here, M is a sufficiently large constant, typically taken as an upper bound of $p_{v,l}$. These constraints ensure that $z_{v,l,d(l),t}$ accurately represents the product $p_{v,l} \bullet x_{v,l,d(l),t}$.

- When $x_{v,l,d(l),t} = 0$, Constraints (C.2) and (C.5) ensure that $z_{v,l,d(l),t} = 0$;
- When $x_{v,l,d(l),t} = 1$, Constraints (C.3) and (C.4) ensure that $z_{v,l,d(l),t} = p_{v,l}$.

Thus, Constraints (C.2) – (C.5) successfully transform the original nonlinear product $z_{v,l,d(l),t} = p_{v,l} \bullet x_{v,l,d(l),t}$ into a set of linear constraints. Therefore Equation (5) can be rewritten as follows:

$$q_{v,l} = \sum_{t \in T} z_{v,l,d(l),t}, \forall v \in V, \forall l \in L_v \tag{C.6}$$

References

[1] IEA, World Energy Outlook 2023, IEA, Paris, 2023.
[2] B. Liu, F. Li, Y. Hou, S. Antonio Biancardo, X. Ma, Unveiling built environment impacts on traffic CO2 emissions using Geo-CNN weighted regression, Transport. Res. Transport Environ. 132 (2024) 104266.
[3] Z. Liu, X. Ma, X. Liu, G. Homem de Almeida Correia, R. Shi, W. Shang, Optimizing electric taxi battery swapping stations featuring modular battery swapping: a data-driven approach, Appl. Sci. 13 (3) (2023) 1984.
[4] J. Cavadas, G. Homem de Almeida Correia, J. Gouveia, A MIP model for locating slow-charging stations for electric vehicles in urban areas accounting for driver tours, Transport. Res. E Logist. Transport. Rev. 75 (2015) 188–201.
[5] H. Wang, D. Zhao, Y. Cai, Q. Meng, G.P. Ong, Taxi trajectory data based fast-charging facility planning for urban electric taxi systems, Appl. Energy 286 (2021) 116515.
[6] Netherlands Enterprise Agency, Electric transport in The Netherlands. https://english.rvo.nl/information/electric-transport, 2022. (Accessed 11 February 2022).
[7] Y. He, Z. Song, Z. Liu, Fast-charging station deployment for battery electric bus systems considering electricity demand charges, Sustain. Cities Soc. 48 (2019) 101530.
[8] Y. Zhou, Q. Meng, G.P. Ong, Electric bus charging scheduling for a single public transport route considering nonlinear charging profile and battery degradation effect, Transp. Res. Part B Methodol. 159 (2022) 49–75.
[9] Beijing Municipal Commission of Transport, Summary of Work in 2023, Beijing Municipal Commission of Transport, Beijing, 2024.
[10] Land Transport Authority, Land Transport Master Plan 2040, Land Trans. Author. Singapore, 2019. https://www.lta.gov.sg/content/ltagov/en/who_we_are/our_work/land_transport_master_plan_2040.html (Accessed 2019).
[11] S. Bellocchi, K. Klöckner, M. Manno, M. Noussan, M. Vellini, On the role of electric vehicles towards low-carbon energy systems: Italy and Germany in comparison, Appl. Energy 255 (2019) 113848.
[12] F. Knobloch, S.V. Hanssen, A. Lam, H. Pollitt, P. Salas, U. Chewpreecha, M.A. J. Huijbregts, J.-F. Mercure, Net emission reductions from electric cars and heat pumps in 59 world regions over time, Nat. Sustain. 3 (6) (2020) 437–447.
[13] X. Liu, P. Plötz, S. Yeh, Z. Liu, X.C. Liu, X. Ma, Transforming public transport depots into profitable energy hubs, Nat. Energy 9 (2024) 1206–1219.
[14] S. Zhuo, X. Zhu, P. Shang, Z. Liu, Y. Yao, F. Liao, Behavior-Adaptive Sync-Flow Framework: integrating frequency setting and passenger routing in oversaturated urban rail transit networks, Transport. Res. E Logist. Transport. Rev. 189 (2024) 103659.
[15] X. Liu, W.-L. Shang, G.H.d.A. Correia, Z. Liu, X. Ma, A sustainable battery scheduling and echelon utilization framework for electric bus network with photovoltaic charging infrastructure, Sustain. Cities Soc. 101 (2024) 105108.
[16] T.H. Shah, A. Shabbir, A. Waqas, A.K. Janjua, N. Shahzad, H. Pervaiz, S. Shakir, Techno-economic appraisal of electric vehicle charging stations integrated with on-grid photovoltaics on existing fuel stations: a multicity study framework, Renew. Energy 209 (2023) 133–144.
[17] J. Liu, M. Li, L. Xue, T. Kobashi, A framework to evaluate the energy-environment-economic impacts of developing rooftop photovoltaics integrated with electric vehicles at city level, Renew. Energy 200 (2022) 647–657.
[18] U. Fretzen, M. Ansarin, T. Brandt, Temporal city-scale matching of solar photovoltaic generation and electric vehicle charging, Appl. Energy 282 (2021) 116160.
[19] R. Fachrizal, M. Shepero, D. van der Meer, J. Munkhammar, J. Widén, Smart charging of electric vehicles considering photovoltaic power production and electricity consumption: a review, eTransportation 4 (2020) 100056.
[20] Y. Wu, S.M. Aziz, M.H. Haque, Vehicle-to-home operation and multi-location charging of electric vehicles for energy cost optimisation of households with photovoltaic system and battery energy storage, Renew. Energy 221 (2024) 119729.
[21] X. Liu, X. Liu, X. Zhang, Y. Zhou, J. Chen, X. Ma, Optimal location planning of electric bus charging stations with integrated photovoltaic and energy storage system, Comput. Aided Civ. Infrastruct. Eng. 38 (11) (2022) 1424–1446.
[22] L.A.L. Zaneti, N.B. Arias, M.C. de Almeida, M.J. Rider, Sustainable charging schedule of electric buses in a University Campus: a rolling horizon approach, Renew. Sustain. Energy Rev. 161 (2022) 112276.
[23] Z. Ye, N. Yu, R. Wei, X.C. Liu, Decarbonizing regional multi-model transportation system with shared electric charging hubs, Transport. Res. C Emerg. Technol. 144 (2022) 103881.
[24] J. Ji, Y. Bie, L. Wang, Optimal electric bus fleet scheduling for a route with charging facility sharing, Transport. Res. C Emerg. Technol. 147 (2023) 104010.
[25] S.S.G. Perumal, R.M. Lusby, J. Larsen, Electric bus planning & scheduling: a review of related problems and methodologies, Eur. J. Oper. Res. 301 (2) (2022) 395–413.
[26] J.A. Manzolli, J.P. Trovão, C.H. Antunes, A review of electric bus vehicles research topics – methods and trends, Renew. Sustain. Energy Rev. 159 (2022) 112211.
[27] Y. Zhou, H. Wang, Y. Wang, B. Yu, T. Tang, Charging facility planning and scheduling problems for battery electric bus systems: a comprehensive review, Transport. Res. E Logist. Transport. Rev. 183 (2024).
[28] K. Liu, H. Gao, Y. Wang, T. Feng, C. Li, Robust charging strategies for electric bus fleets under energy consumption uncertainty, Transport. Res. Transport Environ. 104 (2022) 103215.
[29] Y. Zhou, Q. Meng, G.P. Ong, H. Wang, Electric bus charging scheduling on a bus network, Transport. Res. C Emerg. Technol. 161 (2024) 104553.
[30] H. Ren, Z. Ma, C. Fai Norman Tse, Y. Sun, Optimal control of solar-powered electric bus networks with improved renewable energy on-site consumption and reduced grid dependence, Appl. Energy 323 (2022) 119643.
[31] X. Liu, X. Cathy Liu, Z. Liu, R. Shi, X. Ma, A solar-powered bus charging infrastructure location problem under charging service degradation, Transport. Res. Transport Environ. 119 (2023) 103770.
[32] F. Plenter, F. Chasin, M. von Hoffen, J.H. Betzing, M. Matzner, J. Becker, Assessment of peer-provider potentials to share private electric vehicle charging stations, Transport. Res. Transport Environ. 64 (2018) 178–191.

[33] J. Chen, X. Huang, Y. Cao, L. Li, K. Yan, L. Wu, K. Liang, Electric vehicle charging schedule considering shared charging pile based on Generalized Nash Game, Int. J. Electr. Power Energy Syst. 136 (2022) 107579.
[34] X. Yang, J. Liu, C. Zhuge, A.T.C. Wong, P. Wang, Exploring the potential of sharing private charging posts: a data-driven micro-simulation approach, Sustain. Cities Soc. 100 (2024) 105053.
[35] Z. Jia, K. An, W. Ma, Utilizing electric bus depots for public Charging: operation strategies and benefit analysis, Transport. Res. Transport Environ. 130 (2024) 104155.
[36] S. Zhuo, X. Zhu, P. Shang, Z. Liu, Passenger route and departure time guidance under disruptions in oversaturated urban rail transit networks, Transport. Res. Rec. (2024) 03611981241258747.
[37] B. Sungwoo, K. Alexis, Spatial and temporal model of electric vehicle charging demand, IEEE Trans. Smart Grid 3 (1) (2012) 394–403.
[38] J.A. Domínguez-Navarro, R. Dufo-López, J.M. Yusta-Loyo, J.S. Artal-Sevil, J. L. Bernal-Agustín, Design of an electric vehicle fast-charging station with integration of renewable energy and storage systems, Int. J. Electr. Power Energy Syst. 105 (2019) 46–58.
[39] A. Ingolfsson, E. Akhmetshina, S. Budge, Y. Li, X. Wu, A survey and experimental comparison of service-level-approximation methods for nonstationary M(t)/M/s(t) queueing systems with exhaustive discipline, Inf. J. Comput. 19 (2) (2007) 201–214.
[40] K.A. Alnowibet, H. Perros, Nonstationary analysis of the loss queue and of queueing networks of loss queues, Eur. J. Oper. Res. 196 (3) (2009) 1015–1030.
[41] N. Izady, D. Worthington, Approximate analysis of non-stationary loss queues and networks of loss queues with general service time distributions, Eur. J. Oper. Res. 213 (3) (2011) 498–508.
[42] M. Gallet, T. Massier, T. Hamacher, Estimation of the energy demand of electric buses based on real-world data for large-scale public transport networks, Appl. Energy 230 (2018) 344–356.
[43] X. Liu, S. Yeh, P. Plötz, W. Ma, F. Li, X. Ma, Electric bus charging scheduling problem considering charging infrastructure integrated with solar photovoltaic and energy storage systems, Transport. Res. E Logist. Transport. Rev. 187 (2024) 103572.
[44] G.R. Chandra Mouli, P. Bauer, M. Zeman, System design for a solar powered electric vehicle charging station for workplaces, Appl. Energy 168 (2016) 434–443.
[45] Z. Liu, G. Homem de Almeida Correia, Z. Ma, S. Li, X. Ma, Integrated optimization of timetable, bus formation, and vehicle scheduling in autonomous modular public transport systems, Transport. Res. C Emerg. Technol. 155 (2023) 104306.
[46] S. Zhuo, J. Miao, L. Meng, L. Yang, P. Shang, Demand-driven integrated train timetabling and rolling stock scheduling on urban rail transit line, Transportmetrica: Transport. Sci. (2023) 1–42.
[47] Z. Zeng, What's next for battery-electric bus charging systems, Commun. Transp. Res. 3 (2023) 100094.
[48] C. Zhong, P. Wu, Q. Zhang, Online prediction of network-level public transport demand based on principle component analysis, Commun. Transp. Res. 3 (2023) 100093.
[49] M. Rizki, T.B. Joewono, Y.O. Susilo, Exploring levels of adoption of multi-function transport apps: Transtheoretical model of change on the customer journey of Transport-SuperApp (TSA) users, Commun. Transp. Res. 4 (2024) 100125.